Chapter 17

Silver Nanoparticle Incorporated Titanium Oxide for Bacterial Inactivation and Dye Degradation

Endang Tri Wahyuni and Roto Roto

Additional information is available at the end of the chapter

http://dx.doi.org/10.5772/intechopen.75918

Abstract

This chapter deals with preparation and characterization of silver nanoparticles incorporated in titania or TiO_2-AgNP in short and its performance study as a visible light responsive photocatalyst for bacterial inactivation and dye degradation. The preparation of TiO_2-AgNP performed by several methods including sol-gel, impregnation, precipitation, and photocatalytic deposition is described. Characterizations by XRD, XPS, FTIR, DRUV, and SEM/TEM machines to confirm the formation of the metallic silver nanoparticle, as well as the shape and size, and to follow the interaction between Ag atoms and other atoms in the crystal lattice of TiO_2 are presented. Further, the antibacterial performance and dye degradation activity of TiO_2-AgNP, both under UV and visible light, are described.

Keywords: silver nanoparticle, titania, visible exposure, antibacterial activity, dye photodegradation

1. Introduction

Titanium dioxide (TiO_2) exists in three different crystal structures that are anatase, rutile, and brookite, where rutile is known as the most stable form [1]. The band gap energy of anatase, rutile, and brookite are 3.2, 3.0, 3.2 eV, respectively [1–5]. It means that they can only be activated with UV light irradiation having a wavelength (λ) of 387 nm or lower. Many studies in the area show the use of UV radiation as a photon source for both photocatalytic inactivation of microorganisms [6–11] and dye degradation [12–30].

The titania has been employed as a photocatalyst in several photocatalytic reactions due to its high photoactivity, low cost, low toxicity and good chemical and thermal stability [1–3]. However, its large energy band gap inhibits it from being active under UV light [31–35]. The solar spectrum consists of only 4–5% UV light and around 40% visible light [31]. Therefore, the efficiency of TiO_2 as a photocatalyst under sunlight irradiation is limited.

Modification of TiO_2 to improve the photocatalytic efficiency of TiO_2 under sunlight visible irradiation is necessary. The modification by non-metal [36–51] and metal [52–83] doping on TiO_2 has been attempted. The metal doping agents introduced for TiO_2 are transition metals (Fe, Cu, Cr, Co, and Ni) [52–56] and noble metals (Ag, Au, Pd, and Pt) [57–83]. Among the noble metals, silver has received considerable interest due to its additional potential as an antibacterial agent [84]. The importance of medical applications of metallic silver [85, 86] and antibacterial activity of TiO_2 [6–11] attracts researchers to think of manufacturing silver-doped titania. There are ongoing works related with the use of Ag for possible medical devices [79], dental implants [78, 79], food packagings [80], air conditioning filters, and so on [79]. Some works focus on bacterial inactivation [34, 63] and dye waste treatment under visible light irradiation [66, 67, 81–83]. Hence, the preparation and characterization of the TiO_2-based photocatalyst and its activity are presented.

2. Preparation of TiO_2-AgNP

2.1. Sol-gel

The sol-gel method involves the interaction of titania sol with silver ion the solution, which forms a gel. The gel is heated at a low temperature to evaporate the solvent followed by calcination at high temperature [31, 35, 72, 73, 78, 80, 82, 83]. The main precursor of titania is commonly liquid titanium(IV) isopropoxide (TTiP) with a chemical formula of $Ti(OC_3H_7)_4$ [31, 35, 72, 75], but titanium n-butoxide ($Ti(OC_4H_9)_4$ [82, 83] is also potential. For silver starting material, $AgNO_3$ is frequently employed [31, 72, 75, 77, 80, 82, 83]; however, silver acetylacetonate is also chosen sometime [35].

Titania sol is prepared by mixing TTip solution in ethanol and water accompanied by stirring vigorously at room temperature for about 15 min. During the dissolution of TTip in the ethanol medium, an exchange of propyl group from TTip with ethyl group from the ethanol to yield titania tetra ethoxides takes places by the release of propanol. Titanium tetra ethoxide is hydrolyzed in acidic medium to form sol titanol of $Ti(OH)_4$.

The $AgNO_3$ solution is mixed with ethanol and stirred [31, 72, 75, 77, 80, 82, 83], giving the sol of silver. Finally, the silver sol is added dropwise to the titania sol with stirring, where transparent titania sol changes its viscous yellow solution. The reaction between titania sol and silver sol is commonly written as follows:

$$Ti(OH)_4 + C_2H_5O - Ag \rightarrow Ti(OH)_3 - Ag + C_2H_5OH \quad (1)$$

The viscous sol was heated at about 60°C to evaporate organic solvents to yield dry gel [72]. The dry gel is calcined at about 350°C to produce TiO_2-AgNP powders, according to the reaction (2):

$$4Ti(OH)_3 - Ag + O_2\ (350^\circ C) \rightarrow 4\ TiO_2 - AgNP + 6\ H_2O \quad (2)$$

In the preparation of TiO_2-AgNP photocatalyst by a sol-gel method, some modifications have been done including the use of acetic acid [83], micellar medium [75], spin coating technique [82], with the purpose to improve TiO_2-AgNP photocatalyst characteristics and performance.

2.2. Impregnation method

The synthesis of TiO_2-AgNP by impregnation method is carried out by stirring the solution of $AgNO_3$ mixed with the suspension of TiO_2 in water for 24 h. The solvent is later removed by drying at 150°C followed with calcination of the product at 500°C [68]. Some modifications in the impregnation method such as the use of capping agent [74] and combustion method [63, 64] are also possible.

The modification starts with silver nanoparticles preparation in polyvinylpyrrolidone (PVP) as a capping agent. For this purpose, the $AgNO_3$ solution is added to methanol and is mixed with PVP. The mixture is refluxed for 3 h at 110°C to give a yellow-orange color solution. The solvent was evaporated at 55°C, and the obtained Ag nanoparticles were dispersed into ethanol and thoroughly washed with hexane and ethanol. The Ag nanoparticles are redispersed into the ethanol under sonication, and TiO_2 powder is added to the solution. This mixture is sonicated for 3 h and is dried at 60°C to remove the solvent followed temperature rise to 90°C [74].

The combustion method is carried out by heating a mixture of $AgNO_3$, titanyl nitrate and glycine as fuel in the muffle furnace at 150°C for 2 h [63, 64]. The remaining solid from the combustion is supposed to be TiO_2-AgNP.

2.3. Precipitation

In the precipitation method, titanium tetra-isopropoxide and silver nitrate were used as a source of titanium and silver, respectively. Ag-doped TiO_2 nanocrystalline powder was prepared by controlled addition of TTIP to absolute ethanol with constant stirring to get a clear solution. A sufficient amount of surfactant solutions (1% CTAB +1% SDS) was added to the solution with constant stirring. The aqueous solution of silver nitrate was added to the solution. A solution of aqueous ammonia was added dropwise to the last solution under stirring with the special arrangement at room temperature until the solution pH reaches 8. After complete precipitation, the solid was washed with Millipore deionized water and acetone several times to remove excess of surfactant. The precipitate was kept under microwave irradiation for 20 min. The dried powder was ground and calcined at 300°C for 3 h in a temperature-controlled muffle furnace [68]. Following calcination, the TiO_2-AgNP was obtained.

2.4. Photocatalytic deposition

In this method, the TiO_2 powder is dispersed into ethanol and water, followed by stirring or sonicating for about 15 min to form titania sol. The $AgNO_3$ solution is added to the sol. The mixture is irradiated with UV lamp for a certain period of time along with constant stirring. After a certain time, the solid was separated by filtration and dried at around 300–400°C [31, 33, 67, 69–71, 73, 79, 81]. In this method, when TiO_2 photocatalyst is exposed to UV light, electrons are revealed along with the formation of OH radicals. The electrons will interact with Ag^+ coming from $AgNO_3$ resulting in the reduction reaction of the Ag^+ to form Ag^0 metallic particles. The small particle of Ag^0 can be inserted into the crystal lattices of TiO_2 [67] and/or deposited onto TiO_2 surface to form a small cluster.

2.5. Other methods

There are several other methods for TiO_2-AgNP preparation, including graphene oxidation [57], radiolitic reduction by using γ-ray [61], electrolytic oxidation-reduction [62], and mirror reaction [65].

3. Characterization of TiO_2-AgNP photocatalyst

3.1. The existence of the silver species in TiO_2-AgNP

The content of Ag incorporated in the TiO_2 crystal structure prepared by sol-gel, precipitation and photodeposition can be determined by elemental analyses by X-Ray Fluorescence (XRF) [68, 75], ICP-MS [35] and atomic absorption spectrophotometry (AAS) [83]. In general, the content of Ag formed in TiO_2-AgNP is proportional to the initial concentration of precursors of the $AgNO_3$ solution.

The presence of Ag in the TiO_2-AgNP can be detected by XRD method. It can be carried out by detecting X-ray diffraction pattern evolution with the reference of native TiO_2. The XRD pattern of TiO_2 recorded by using a Cu$K\alpha$ source of XRD machine gives several characteristics peaks of 2θ values at 25.091, 37.651, 48.021, 53.891, 55.071, 62.381, 68.701, 70.041 and 75.001. These peaks are confirmed with JCPD Card No. (21-1272) and are attributed to the diffraction of TiO_2 anatase. They correspond to the lattice planes (101), (004), (200), (105), (211), (204), (220), (220), and (215), respectively [67, 68, 77, 82]. In many instances, Ag is not detected in the XRD pattern. It is probably located in bulk (inside the TiO_2 crystals) [77], and/or Ag clusters smaller than 0.3 nm [66], or diffused in the TiO_2 crystal lattice [68], or well dispersed throughout the TiO_2 surface [31] (**Figure 1**).

High Ag content (more than 0.25 mol%) in TiO_2-AgNP prepared by precipitation assisted with microwave [68] and that of by photocatalytic reduction [67] have additional diffraction peaks at 2θ values of 38.011, 44.261, 64.021 and 77.361. The appearance of the peaks can be assigned to the face centered cubic lattice planes of metallic silver of (111), (200), (200) and (311) planes, respectively [67, 68]. It is evident that TiO_2-AgNP photocatalyst with low metallic Ag content is undetectable by the XRD technique [82]. The detectable metallic Ag level

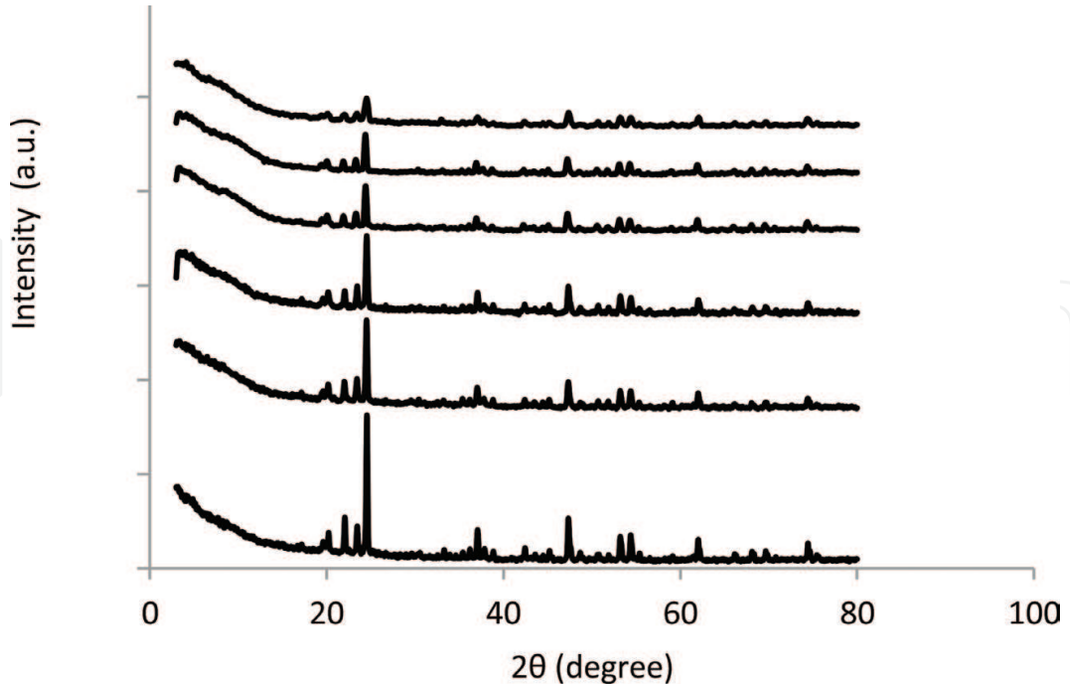

Figure 1. XRD patterns of (a) TiO_2, (b) TiO_2/Ag-0.05%, (c) TiO_2/Ag-0.10%, (d) TiO_2/g-0.15%,(e) TiO_2/Ag-0.25%, and (f) TiO_2/Ag-0.50% [71].

is found to be more than 0.80 moles% [66], but 0.25 moles% or higher is also reported [68]. Depending on the concentration, the detectable metallic silver in TiO_2-AgNP is also observed in the XRD pattern when TiO_2-AgNP is calcined at a higher temperature (700°C) since sintering step causes Ag particles to form large aggregate [31].

The valence state of silver, as ionic Ag^+ or metallic silver Ag^0, in the TiO_2-AgNP photocatalyst can be distinguished by XPS. The XPS spectrum shows the characteristic Ag 3d peak that has a binding energy of 368 eV with a 6.0 eV splitting of the 3d doublet of low spin $3d^{1/2}$ and high spin $3d^{5/2}$ [33]. It confirms that the presence of metallic silver deposits on the TiO_2 [33]. It is different from the XRD data that can only provide the metallic silver in high level; the XPS gives additional proof that the metallic silvers are formed in TiO_2-AgNP at all concentration levels.

The existence of Ag in TiO_2-AgNP can also be distinguished by temperature-programmed reduction (TPR) spectrometry technique. The profile of the TPR spectra of sol-gel TiO_2-AgNP calcined at 350°C [72] shows reduction peak at around 135°C, which suggests a reduction of Ag^+ into Ag^0 metallic without interacting with the support. Also, TiO_2-AgNP calcined at 500°C give spectra peak at around 350 and 500°C, probably due to Ag reduction with support material [72].

3.2. Band gap energy (Eg) and absorption edge (λ) of TiO_2-AgNP

3.2.1. Mechanism and role of Ag in TiO_2-AgNP on the absorption shift into visible light

The incorporation of Ag on TiO_2 is meant to allow the TiO_2 to be active under visible light. The photocatalytic ability of TiO_2 photocatalyst under visible is assigned by the lower band gap energy (Eg) or absorption in visible light. The band gap energy (Eg) can be determined based

on the data of the maximum absorption wavelength (λ) according to the equation Eg = 1239/λ, where the maximum absorption wavelength is obtained from the diffuse reflectance (DR) data [67].

The DR-spectra at 200–800 nm of TiO_2 displays that the maximum absorption is seen at around 400–390 nm corresponding to 3.15–3.20 eV of the band gap energy of anatase [1–3]. Furthermore, the metallic silver loading on TiO_2 is observed to shift the maximum absorption to a longer wavelength that is about 430–574 nm [31, 66, 67, 72, 75, 81]. The DR spectra give respective band gap energy as much as 2.88–2.16 eV. The absorption wavelength or the band gap energy values allow the TiO_2-AgNP photocatalyst to be active in the visible region. The absorption shift may be resulted by the diffusion of the metallic silver into the crystal lattice of the TiO_2 structure that the silver to be dispersed or inserted between the conduction and valence bands of the host material [31, 67, 75] (**Figure 2**).

The absorption shift is found to be affected by Ag content in TiO_2-AgNP [67, 68, 75, 81], the preparation method of TiO_2-AgNP, and calcination temperature [72]. The shift increases with the increasing Ag amount in TiO_2 because more Ag inserted into the gap so that the gap becomes narrower than that of bare TiO_2, shifting in the absorption wavelength to increase. Based on the preparation method, TiO_2-AgNP photocatalyst prepared by sol-gel has a more substantial shift in the wavelength than the ones produced by the impregnation method [72]. In the sol-gel process, the silver ion (Ag^+) having a small size interacts with the titania sol, allowing the ion to disperse into the crystal lattice of TiO_2. Meanwhile, in the impregnation the silver introduced into the titania sol present as $AgNO_3$ salt is difficult to penetrate the lattice [75], giving less effect on the band gap. The final step in the TiO_2-AgNP preparation

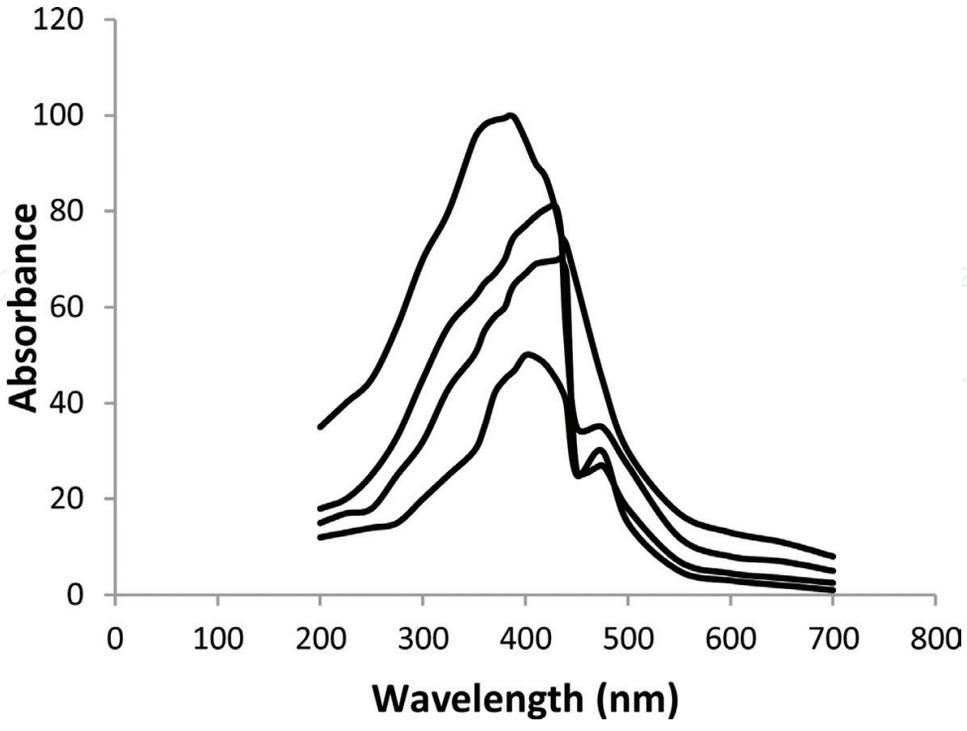

Figure 2. DR spectra, from the top in order representing TiO_2, TiO_2/Ag-0.05%, TiO_2/Ag-0.25%, and TiO_2/Ag-0.50% [71].

process is calcination at a higher temperature that is about 350–500°C. The high calcination temperature of TiO_2-AgNP gives smaller absorption shift than the low calcination temperature [72]. With a high temperature, the silver sintering on TiO_2 may be occurred to form bigger Ag metallic cluster, which prevents it from entering the gap. The significant shift of the absorption wavelength is expected because this should promote higher photocatalyst activity in the visible region.

The diffusion of Ag into the crystal lattice of TiO_2 may enlarge its basal spacing (d) that can be confirmed by their basal spacing obtained from the XRD patterns. It is found that the presence of Ag in the TiO_2-AgNP causes the XRD peak position of TiO_2 shifts to a low 2θ angle. Further, the 2θ angle position is getting lower as the Ag content increases. The 2θ angle value is related to the basal spacing (d) of TiO_2 crystal as represented by Bragg's equation [68]:

$$n\lambda = 2\,d\sin\theta \tag{3}$$

The equation describes the smaller sin θ value, the larger the d spacing. It is known that the value of d increases gradually with increase in Ag contents. The enlargement of the XRD basal spacing (d) implies that more silver diffuses into the lattice of TiO_2 [68]. As the Ag contents increasing from 0 to 0.25 mol%, the peak broadening of [101] planes gradually increases, which indicates the smaller crystallite size of Ag. The smaller size facilitates them to diffuse into the crystal lattice easily.

The insertion of the metallic silver into the TiO_2 crystal lattice may distort the structure of TiO_2 or disturb the chemical bonds of Ti-O in the solid. To better understand the effect of the Ag as a doping agent, the spectrometer data of IR is used. The FTIR spectra of both TiO_2 and TiO_2-AgNP photocatalyst illustrating several absorptions appear at various wavelengths [68, 77, 81]. A broad peak at 3448 cm^{-1} represents O-H stretching of Ti-O-H. Also, a peak seen at 1635 cm^{-1} is due to the OH bending mode of water adsorbed on the surface of TiO_2. The peaks at the wavelength of 540 and 678 cm^{-1} are also observed due to Ti-O-Ti stretching and Ti-O-Ti bending, respectively [68, 75]. After loading Ag on TiO_2, the peaks at 540 and 679 cm^{-1} shifts to 556 and 694 cm^{-1}, respectively. The shifts may be affected by the interaction between Ag and TiO_2 to form Ti-O-Ag composite and/or the insertion of Ag into host lattice of TiO_2 [68].

The XRD patterns confirm the distortion of the TiO_2 structure after doping with metallic Ag. The XRD peaks belonged to both TiO_2 and TiO_2-AgNP seemed similar, but the peak intensity decreases after Ag loading. The intensity decreases imply the alteration of the crystallinity due to the insertion of Ag into the lattice of the TiO_2 crystal [67].

3.3. Particle size of the silver on TiO_2-AgNP

The Ag incorporation into the TiO_2 may affect several important properties including particle size and surface area. The particle size determines its surface area, where the smaller the grain size, the larger the surface area. TEM can trace the particle size of Ag in TiO_2-AgNP. The TEM image displays that the size varied with the Ag content in the TiO_2-AgNP [33, 67]. For the two atomic% Ag in TiO_2-AgNP sample, Ag deposits are well dispersed on the TiO_2 particles with an average particle size of 2–4 nm. At high silver level, the formation of large Ag

particles (>100 nm) is observed in the TEM images [33, 67]. The particle size of Ag-doped TiO_2 is also directed by the preparation methods [33]. In TiO_2-AgNP prepared by the impregnation method, Ag is detected to have a larger size than that of sol-gel. In the impregnation process, $AgNO_3$ salt and TiO_2 are suspended in water in the TiO_2-AgNP preparation [33]. Consequently, the Ag particle is not limited by the TiO_2 structure that enables them to form a large agglomerate. Meanwhile, in the sol-gel method, TiO_2-AgNP is prepared from titania sol and Ag^+ solution that allows them to have mutual interaction and inhibit their particle growth. As a result, it forms the small grain size (**Figure 3**).

3.4. Surface area of TiO_2-AgNP

The surface area is determined by surface area analyzer based on the BET method. In general, the surface area of TiO_2-AgNP is controlled by the Ag content in TiO_2-AgNP, preparation method, and the calcination temperature [33, 68, 72]. The surface area of TiO_2-AgNP prepared by impregnation method is observed to decrease with increase in the Ag-doped TiO_2 [72]. By impregnation method, the metallic silver is formed as large agglomerate that may block the surface of the TiO_2 particle. Such surface blocking leads to the surface area to decline. In contrast, by a sol-gel method, the surface area increases with the enlargement of Ag content in TiO_2-AgNP. The particle size of the metallic Ag is small due to the limitation of particle growth.

By the photo-deposition method, the addition of Ag at only 0.25 mol%, an appreciable increase in the specific surface area is observed [33, 68]. The surface area of TiO_2-AgNP with Ag content smaller than 0.25 mol% is not significantly different from that of the pure TiO_2 due to the vast and thin dispersion of the Ag particles on the TiO_2 structure. Ag in TiO_2-AgNP as much as 0.25 mol% seems to be well dispersed on the surface of the TiO_2 grain that contributes to a large surface area. The Ag loading higher than 0.25 mol% leads to the decrease in surface area that is resulted from by large silver aggregate.

The other reasons for the surface area improvement are proposed as follows [31, 68, 76]. The Ag doping with a suitable amount (ca. 2–6 mol%) promotes the phase transformation of TiO_2 from anatase to rutile since the surface area of rutile is larger than that of the anatase. The Ag-doped TiO_2 also has a depressing effect on the anatase grain growth. The average crystallite

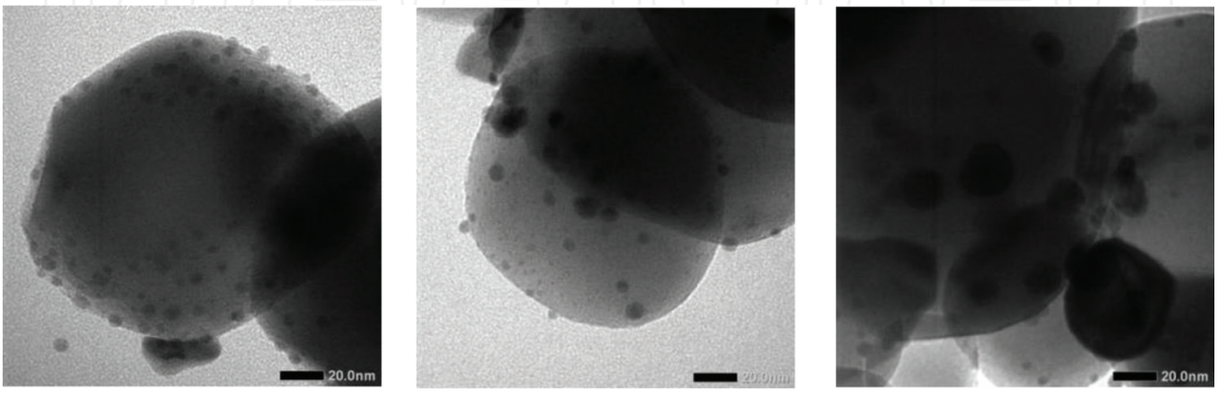

Figure 3. The TEM images of (a) TiO_2/Ag-0.05%, (b) TiO_2/Ag-0.25%, and (c) TiO_2/Ag-0.50% [71].

size of the TiO_2 can be calculated by using the Scherrer's Equation [31]. It is observed that the TiO_2 crystallite has an average size of 15 nm, and it decreases up to 10 nm for 0.25 mol% of Ag loading [68]. It is also confirmed that the decreasing the crystallite size increases the specific surface area of the TiO_2 powder.

4. Activity of TiO_2-AgNP photocatalyst

The doping TiO_2 with metallic Ag is intended to activate TiO_2-AgNP photocatalyst under visible light both for bacterial inactivation and dye photodegradation.

4.1. Bacterial inactivation

The doping TiO_2 with metallic silver to produce TiO_2-AgNP has been investigated as a potential antibacterial agent in inactivating *Escherichia coli* [63–65, 78, 79] under visible light exposure. The TiO_2-AgNP exposure to UV light for bacterial inactivation is also essential.

TiO_2-AgNP demonstrates a significant activity in the bacterial inactivation under visible light. The antibacterial performance of TiO_2-AgNP is found to be higher than that of unmodified TiO_2. Both TiO_2 and TiO_2-AgNP can kill bacteria because TiO_2 provides OH radicals during UV or visible irradiation at a suitable wavelength. The OH radicals attack and destroy the bacterial wall [10, 11]. Under visible light, TiO_2-AgNP can be activated since TiO_2-AgNP has a low band gap energy (Eg) that matches with the visible region wavelength. Meanwhile, due to its high band gap energy (Eg), which is in the same order as UV light, TiO_2 is less active under visible light. Addition of Ag to TiO_2 also gives the excellent antibacterial agent, that is by penetrating the metallic Ag nanoparticles into the cell membrane of the bacteria [84]. There is a synergic effect of TiO_2 and Ag in inhibiting bacteria [63–65, 78, 79]. The activity of Ag in the bacteria inactivation process is examined by applying TiO_2-AgNP in dark condition [81]. It has been postulated that silver disrupts the cell wall and affects the rapid penetration of the metallic ions into the cell where irreversible precipitation of the bacteria's DNA occurs [84].

The role of Ag in TiO_2-AgNP in the bacterial inhibition under visible light is affected by its ability as a center of the separation of photoinduced electron and OH radicals that delay the recombination of electron and hole [34, 63–65, 78, 79]. The other role of Ag in the improving the bacterial inactivation corresponds to the electron capture that can prevent the recombination. The inhibition of the recombination creates more OH radicals, which improves the bacterial inactivation.

The Ag content in TiO_2-AgNP is subjected to test further. Increase in Ag content leads to decline in bacterial inactivation [34, 63–65, 78, 79]. Increasing Ag in TiO_2-AgNP can enhance the electron capture, forming anion Ag, which allows more OH radical available. The more OH radicals available, the better bacterial inactivation. However, a further increase in Ag content can block the TiO_2 surface and prevent the light absorption, producing a lower amount of OH radicals. The other possible reason is the attachment of OH radical with excess Ag anion. The depletion of OH radicals leads to the inactivation declined [64].

Comparing between the bacterial inactivation under UV and visible light with and without photocatalyst, it is similar to the UV photolysis system [63, 64]. Visible light photolysis alone is observed to play a role in microorganism inactivation. The bacterial inactivation in UV-A or visible light is observed due to the synergetic effects of radiating energy and mild heat produced during the irradiation [63]. In the presence of TiO_2-AgNP photocatalyst, it is found the rates of inactivation were higher in the presence of UV than that of visible light.

UV light has germicidal property, and TiO_2 itself possesses higher photocatalytic activity in UV region due to its large band gap energy. On the other hand, doping with metal is mainly done to extend the absorbance of TiO_2 to the visible region. Therefore, the photocatalytic inactivation in the presence of UV light and TiO_2: Ag catalyst is a synergetic effect of antimicrobial property of silver, the germicidal property of UV and photocatalytic activity of the TiO_2 photocatalyst [63, 64]. It should be noted that the antibacterial inactivation is dependent on several operating conditions such as visible light intensity and catalyst amount.

4.1.1. Effect of visible light intensity

Photocatalytic inactivation reactions are highly dependent on the irradiation intensity of the light source [34, 63]. The increase in the visible light intensity from 2 to 8 $W.m^2$ can enhance the bacterial inactivation over TiO_2-AgNP photocatalysts. The observed enhancement in the inactivation is due to the increase in the number of photons produced as light intensity rise.

4.1.2. Effect of the photocatalyst dose

The addition of catalyst to the solution resulted in a better bacterial inactivation than the control experiments. At low catalyst dose (0.1 g/L), the observed inactivation was not significant because of less availability of OH radicals to target a large number of bacteria. The increase in the photocatalyst dose to 0.25 g/L shows the possibility of an increase in the number of OH radicals sufficient enough to target the microorganism number, which improves bacterial inactivation. At 0.25 g/L, the maximum inactivation shows the maximum availability of OH radicals in the solution. When the photocatalyst loading is increased above 0.25 g/L, the inactivation process becomes slow where more bacterial colonies are detected for photocatalyst loading of 0.5 and 1.0 g/L. A high amount of catalyst in the solution results in turbidity increase that blocks the radiation to reach to microorganisms and other catalyst particles (shadowing or screening effect), which leads to a low rate of inactivation. The similar effect is observed for the UV photocatalytic inactivation [63, 64].

4.1.3. Effect of pH

It is reported that the inactivation of bacteria was not influenced by changing the pH of the solution. The rate constant also remains constant for all pH range [64]. The zero point of charge (ZPC) for TiO_2-AgNP and *E. coli* can be estimated as ZPC (TiO_2-AgNP) = 4.0 and ZPC (*E. coli*) = 2.5, respectively. At all the pH values studied, both *E. coli* and the catalyst had a negative surface charge. Therefore, the electrostatic repulsion between bacterial cells and catalyst particles could result in the similar inactivation effect.

4.2. Dye degradation

The performance of TiO_2-AgNP photocatalyst is investigated for dye photodegradation under visible light. Among dyes studied as examples in photodegradation test include methylene blue [31, 66], rhodamine-B (RD-B) [33], and acid read 8S [67].

4.2.1. The activity of TiO_2-AgNP photocatalyst under visible light

TiO_2-AgNP photocatalyst shows higher activity under visible light in the photodegradation of dyes than that of bare TiO_2 [33, 31]. It means that TiO_2-AgNP is also photoactive in the visible region. The energy of the visible light (2.2–3.0 eV) is near the band gap energy of TiO_2-AgNP, which is about 2.7–2.9 eV [72, 75]. The visible light is required to activate TiO_2-AgNP for the dye photodegradation. The energy of the visible light is slightly lower than the band gap of TiO_2 anatase (3.2 eV) and TiO_2 rutile (3.0 eV). The visible light is unable to excite an electron in TiO_2. Therefore, the photocatalytic performance of TiO_2 is weak.

Increasing Ag content in TiO_2-AgNP promotes photodegradation as shown in many works. But further increase in Ag content could have a detrimental effect on the photodegradation result [31, 33, 66, 68]. The optimum Ag content in TiO_2-AgNP is found be at about 2.5 w% [33], 0.80% mol [66], and 0.25 mol% [68].

The effect of Ag content in TiO_2-AgNP on photocatalytic activity can be explained as follows. The appropriate amount of Ag-doped TiO_2 allows effective capture of the photoinduced electrons [31, 33, 66, 67]. The photoinduced electrons during light irradiation results in negatively charged Ag. The photoinduced electrons can be immediately transferred to oxygen atoms of TiO_2. The electron transfer from the TiO_2 conduction band to metallic silver particles at the interface is thermodynamically favorable because the Fermi level of TiO_2 is higher than that of silver metals [31, 33]. It results in the formation of the Schottky barrier at metal-semiconductor contact region, which improves the charge separation. Accordingly, the recombination of the electron and the OH radicals can be inhibited more [33]. This condition explains the significant enhancement of the photocatalytic activity of TiO_2-AgNP. The increase in Ag content will keep the photodegradation improve until it reaches its optimum.

At high Ag loading above its optimum level, an excess amount of negatively charged silver species are available. A significant amount of the negatively charged silver particles allows silver atoms to attract more OH radicals. However, it reduces charge separation efficiency [31, 35, 66] or raises electron-hole recombination and decrease dye photodegradation. Another possible reason is the formation of silver metallic clusters inside the TiO_2 crystal. The metal clusters give small contact surface area of the photocatalyst. The atomic Ag in TiO_2-AgNP may act as a barrier to obstruct light absorption by titania. It also prevents organic substrates from contacting the photocatalyst surface. Silver atoms may become media for electron-hole recombination [44]. As a result, they reduce photodegradation reaction.

4.2.2. The performance of TiO_2-AgNP under UV light in the dye photodegradation

The photocatalyst working under the UV light is frequently assessed for dye photodegradation such as methyl orange [68], diazo type dye of DR 23 and DB 53 [69, 70] and methylene

blue [74, 82]. It is evident that in the presence of Ag, the photocatalytic performance of the TiO_2-AgNP under UV light improves. The photocatalytic activity of TiO_2-AgNP under the UV light is higher than that of unmodified one. The role of the Ag in the improvement of the dye photodegradation under UV light can explain similarly to the effect of Ag under visible light.

The photodegradation performance of TiO_2-AgNP under visible light is better than under UV light. In the case of rhodamine-B degradation, the dye can be adsorbed by Ag particle in TiO_2-AgNP. The dye adsorbed on the Ag surface can be activated by visible light because the dye absorbs the electromagnetic radiation in the range of visible light. The activated dye molecules are unstable and start to degrade. On the one hand, the lower UV light photocatalytic activity of TiO_2-AgNP may be due to surface plasmon resonance of metallic Ag that reduces UV light excitation [66]. This unexcitability of the photocatalyst leads to the low dye photodegradation.

4.2.3. Effect of the process conditions

The dye photodegradation of dye by TiO_2-AgNP under UV light is controlled by the level of Ag in photocatalysts and irradiation light. Also, the effectiveness of the dye photodegradation is affected by operating conditions such as photocatalyst dose, initial concentration, contact time and solution pH.

4.2.3.1. The effect of the photocatalyst dose

The dye photodegradation increases with the increase in the photocatalyst dose. The effectiveness of the photodegradation reduces when the photocatalyst dose is further increased [66–68, 81]. The maximum photodegradation is obtained by using 1 g photocatalyst/100 mL [68, 74, 81]. In other work, the use of 0.6 g photocatalyst/L is also reported [67]. Such data can be explained based on the number of active sites available for photocatalytic reactions. More active sites of the photocatalyst are available when the dose of the photocatalyst increases. However, the use of a large number of photocatalysts may cause agglomeration of the material to produce big particle size. The large particle size gives small surface area, which decreases the number of active sites on the surface [36, 38]. Another reason for the decrease in the degradation can be attributed to the increase in the turbidity of suspension due to more suspended photocatalyst solids. The light scattering by the catalyst particles leads to the blockage of photon absorption. Moreover, less OH radicals can be created [1, 2].

4.2.3.2. Effect of initial pH

In the acidic pH, the effectiveness of the dye photocatalytic degradation over TiO_2-AgNP is found to be low. The photodegradation improves as pH increasing, but when the pH is increased further the photodegradation declines. For methyl orange photodegradation, the optimum pH is reached at 3 [68]. The dye degradation over heterogeneous photocatalyst of TiO_2 is initiated by adsorption on photocatalyst surface, leading to sequentially or simultaneously dye degradation. The effectiveness of the adsorption and degradation of dye depends on the surface charge of the catalyst and solution pH. The pH is an effective parameter to

affect the surface state [68, 74]. The amphoteric characteristics of synthesized oxides influence the surface charge of the photocatalyst. The pH of dye solution varies with the surface charge of the photocatalyst and shifts the position of redox reaction [68, 74]. Based on the amphoteric characteristics of TiO_2, the following equilibriums take place:

$$Ti-OH + H^+ \rightleftarrows Ti-OH_2^+ \quad (4)$$

$$Ti-OH + OH^- \rightleftarrows Ti-O^- + H_2O \quad (5)$$

Concerning the reactions (4) and (5), it is evident that the surface of the photocatalyst can become positively charged in acidic medium and negatively charged in alkaline medium. On the other side, methyl orange in the aqueous medium is in the anionic state that can also affect the adsorption.

At pH lower than 3, the H^+ ions cause the dye to become positively charged. Note that the surface of the catalyst is also positive. Since both dye and photocatalyst are positively charged, it will inhibit adsorption and photodegradation. At pH 3, the dye becomes anionic, while the photocatalyst surface is still positively charged. It facilitates better electrostatic attraction between dye molecules and positively charged photocatalyst surface, which speeds up the photodegradation. At pH greater than 7, the surface of the photocatalyst has become negatively charged, which leads to electrostatic repulsion between methyl orange and photocatalyst. Therefore, it results in a decrease in the dye photodegradation efficiency [68].

Different from the anionic dye, a cationic dye such as methylene blue shows the maximum adsorption and photodegradation at neutral to basic pH. At low pH, the photodegradation may occur less efficient due to electrostatic repulsion between methylene blue molecules and photocatalyst, since both dye molecules and photocatalyst have positive charges. The electrostatic repulsion can inhibit adsorption that results in a decline in the dye degradation. In neutral pH, the dye species is positively charged, whereas photocatalyst is neutral so that they create electrostatic interaction. At higher pH, the dye is neutral, whereas the photocatalyst is in the anionic state, which facilitates efficient adsorption and photodegradation [68]. The maximum photodegradation for this dye takes place at pH 9 [74].

4.2.3.3. Effect of the initial dye concentration

It is apparent that the dye photodegradation reduces gradually when dye concentration improves [66, 75]. At low dye concentration, a few dye molecules in solution can move freely into the active surface of the photocatalyst. When the abundant active sites of the photocatalyst are available to absorb the dye, the dye photodegradation becomes efficient. High dye concentration gives more dye molecules that hinder their movement close to the photocatalyst. Therefore, the adsorption and the photodegradation decrease. For the photocatalyst, the surface has been occupied by much dye that diminishes the active sites at the surface. It leads to less dye adsorption and declines photodegradation [66, 74, 75].

4.2.3.4. Effect of the irradiation time

The UV light irradiation time can represent: (1) how long the photocatalyst contact with irradiating light, for further formation of OH radicals and (2) how long the contact between dye with OH radicals to proceed photodegradation. A general trend shows that the extension of the irradiation time enhances photodegradation, but the photodegradation stays constant or even decreases slightly for extended irradiation. Long UV light exposure produces more OH radicals, which helps the photodegradation take place more efficiently. However, further addition of irradiation time leads to surface saturation of the photocatalyst to release OH radicals [66, 75].

Author details

Endang Tri Wahyuni* and Roto Roto

Address all correspondence to: endang_triw@ugm.ac.id

Chemistry Department, Faculty of Mathematics and Natural Sciences Gadjah Mada University, Yogyakarta, Indonesia

References

[1] Hoffmann MR, Martin ST, Choi W, Bahnemann DW. Chemical Reviews. 1995;**95**:69-96

[2] Linsebigler AL, Guangquan LJ Jr, Yates T. Chemical Reviews. 1995;**95**:735-758

[3] Nakata K, Fujishima A. Journal of Photochemistry and Photobiology C: Photochemistry Reviews. 2012;**13**:169-189

[4] Fujishima A, Rao TN, Tryk DA. Journal of Photochemistry and Photobiology C. 2000;**1**:1-21

[5] Mills A, O' Rourke C, Moore K. Journal of Photochemistry and Photobiology A: Chemistry. 2015;**310**:66-105

[6] Caballero L, Whitehead KA, Allen NS, Verran J. Journal of Photochemistry and Photobiology A. 2009;**202**:92-98

[7] Cai R, Hashimoto K, Itoh K, Kubota Y, Fujishima A. Bulletin of the Chemical Society of Japan. 1991;**4**:1268-1273

[8] McCullagh C, Robertson J, Bahnemann D, Robertson P. A review. Research on Chemical Intermediates. 2007;**33**:359-375

[9] Peller JR, Whitman RL, Griffith S, Harris P, Peller C, Scalzitti J. Journal of Photochemistry and Photobiology, A: Chemistry. 2007;**186**:212-217

[10] Kiwi J, Nadtochenko V. Langmuir. 2005;**21**:4631-4641

[11] Foster HA, Ditta IB, Varghese S, Steele A. Applied Microbiology and Biotechnology. 2007;**90**:1847-1868

[12] Sökmen M, Özkan A. Short communication. Journal of Photochemistry and Photobiology A: Chemistry. 2002;**147**:77-81

[13] Akpan UG, Hameed BH. A review. Journal of Hazardous Materials. 2009;**170**:520-529

[14] Mukhlish MZB, Najnin F, Rahman MM, Uddin MJ. Journal of Scientific Research. 2013;**5**(2):301-314

[15] Tayade RJ, Surolia PK, Kulkarni RG, Jasra RV. Science and Technology of Advanced Materials. 2007;**8**:455-462

[16] Reza KM, Kurny ASW, Gulshan F. A review. Applied Water Science. 2017;**7**:1569-1578

[17] Markovic D, Jokic B, Saponjic Z, Potkonjak B, Jovancic P, Radetic M. Clean – Soil, Air, Water. 2013;**41**(10):1002-1009

[18] Joseph C, Sharain-Liew YL, Bono A, Teng LY. Asian Journal of Chemistry. 2013;**25**(15): 8402-8406

[19] Ahmed MA, El-Kator EE, Gharni ZH. Journal of Alloys and Compounds. 2013;**553**:19-29

[20] Li R, Jia Y, Bu N, Wu J, Zhen Q. Journal of Alloys and Compounds. 2015;**643**:88-93

[21] Ajmal A, Majeed I, Malik RN, Idriss H, Nadeem MA. A comparative overview. RSC Advances. 2014;**4**:37003-37026

[22] Zuo R, Du G, Zhang W, Liu L, Liu Y, Mei L, Zhaohui LZ. Hindawi publishing corporation. Advances in Materials Science and Engineering. 2014:1-7

[23] Mehra M, Sharma TR. Advances in Applied Science Research. 2012;**3**(2):849-853

[24] Gautam A, Kshirsagar A, Biswas R, Banerjee S, Khann PK. RSC Advances. 2016;**6**:2746-2759

[25] Giwa A, Nkeonye PO, Bello KA, Kolawole KA. Journal of Environmental Protection. 2012;**3**:1063-1069

[26] Carcel RA, Andronic L, Duta A. Journal of Nanoscience and Nanotechnology. 2011; **11**(10):9095-9101

[27] Subramani AK, Byrappa K, Anand S, Lokanatha Rai KM, Ranganathaiah C, Yoshimura M. Bulletin of Materials Science. 2007;**30**(1):37-41

[28] Khataee AR, Kasiri MB. Journal of Molecular Catalysis A: Chemical. 2010;**328**(1-2):8-26

[29] Neppolian B, Choi HC, Sakthivel S, Arabindoo B, Murigusen V. Journal of Hazardous Materials. 2002;**89**(2-3):303-317

[30] Mahadwad OK, Jasra RV, Parikh PA, Tayade RJ. Journal of Environmental Science & Engineering. 2010;**52**(3):181-184

[31] Seery MK, George R, Floris P, Pillai SC. Journal of Photochemistry and Photobiology A: Chemistry. 2007;**189**:258-263

[32] Pelaez M, Nolan NT, Pillai SC, Seery MK, Falaras P, Konto AG, Dunlop PSM, Hamilton JW, Byrne JA, O'shea K, Entezari MH, Dionysiou DD. Applied Catalysis B: Environmental. 2012;**125**:331-349

[33] Sung-Suh HM, Choi JR, Hah HJ, Koo SM, Bae YC. Journal of Photochemistry and Photobiology A: Chemistry. 2004;**163**:37-44

[34] Sontakke S, Mohan C, Modak J, Madras G. Chemical Engineering Journal. 2012; **189-190**:101-107

[35] Colmenares JC, Aramedia MA, Marinas A, Marinas JM, Ubano FJ. Applied Catalysis A: General. 2006;**306**:120-127

[36] Cong Y, Zhang J, Chen F, Anpo M. Journal of Physical Chemistry C. 2007;**111**(19):6976-6982

[37] Yates HM, Nolan MG, Sheel DW, Pemble ME. Journal of Photochemistry and Photobiology A: Chemistry. 2006;**179**:213-223

[38] Cheng X, Yu X, Xing Z, Wan J. Energy Procedia. 2012;**16**:598-605

[39] Cheng X, Yu X, Xing Z, Yang L. Arabian Journal of Chemistry. 2016;**9**:1706-1171

[40] Mekprasart W, Pecharapa W. Energy Procedia 9th Eco-Energy and Materials Science and Engineering Symposium. 2011;**9**:509-514

[41] Nassoko D, FangLi Y, Wang H, Li J-L, Li Y-Z, Yu Y. Journal of Alloys and Compounds. 2012;**540**:228-235

[42] Ananpattarachai J, Kajitvichyanukul P, Seraphin S. Journal of Hazardous Materials. 2009;**168**(1):253-261

[43] Zhou X, Peng F, Wang H, Yu H, Yang J. Materials Research Bulletin. 2011;**46**(6):840-844

[44] Devi LG, Kavitha R. Materials Chemistry and Physics. 2014;**143**(3):1300-1308

[45] Rockafellow EM, Stewart LK, Jenks WS. Applied Catalysis B: Environmental. 2009;**91**(1-2):554-562

[46] Szatmáry L, Bakardjieva S, Šubrt J, Bezdičkza P, Jirkovský J, Bastl Z, Brezová V, Korenko M. Catalysis Today. 2011;**161**(1):23-28

[47] Yu J, Liu S, Xiu Z, Yu W, Feng G. Journal of Alloys and Compounds. 2009;**471**(1-2):23-25

[48] Lu J, Dai J, Guo M, Yu L, Lai K, Huang B. Applied Physics Letters. 2012;**100**:102114

[49] Hiroshi I, Yuka W, Hashimoto Kazuhito H. Chemical Letters. 2003;**32**(8):772-773

[50] Yu S, Yun HY, Kim YH, Yi J. Applied Catalysis B: Environmental. 2014;**144**:893-899

[51] Yang Y, Ni D, Yao Y, Zhong Y, Ma Y, Yao J. RSC Advances. 2015;**5**:93635-93643

[52] Morikawa T, Irokawa Y, Ohwaki T. Applied Catalysis A: General. 2006;**314**:123-127

[53] Zhu J, Chen F, Zhang J, Chen H, Anpo M. Journal of Photochemistry and Photobiology, A: Chemistry. 2006;**180**(19):196-204

[54] Siddhapara KS, Shah DV. Advances in Materials Science and Engineering. 2014;**4**

[55] Khakpash N, Simchi A, Jafari T. Journal of Materials Science: Materials in Electronics. 2012;**23**:659-667

[56] Yang S, Lee H. Nanoscale Research Letters. 2017;**12**:582

[57] Razali MH, Ahmad-Fauzi MN, Mohamed AR, Sreekantan S. International Journal of Materials, Mechanics and Manufacturing. 2013;**1**(4)

[58] Ribao P, Maria J, Rivero MJ, Ortiz I. Environmental Science and Pollution Research. 2017;**24**:12628-12637

[59] Adán C, Marugán J, Obregón S, Colón G. Catalysis Today. 2015;**240**:93-99

[60] Batalović K, Bundaleski N, Radaković J, Abazović N, Mitrić M, Silva RA, Savić M, Belošević-Čavor J, Rakočević Z, Rangel CM. Physical Chemistry Chemical Physics. 2017;**19**:7062-7071

[61] Enachia M, Guixb M, Branistea T, Postolachea V, Ciobanua V, Ursakic V, Schmidtb OG, Tiginyanu I. Электронная обработка материалов (in English). 2015;**51**(1):3-8

[62] Grabowska E, Remita H, Zalezka A. Physicochemical Problems of Mineral Processing. 2010;**45**:29-38

[63] Maicu M, Hidalgo MC, Colón G, Navío JA. Journal of Photochemistry and Photobiology A: Chemistry. 2011;**217**:275-283

[64] Sontakke S, Modak J, Madras G. Chemical Engineering Journal. 2010;**165**:225-233

[65] Sontakke S, Modak J, Madras G. Applied Catalysis B: Environmental. 2011;**106**:453-459

[66] Li Y, Ma M, Chen W, Li L, Zen M. Materials Chemistry and Physics. 2011;**129**:501-505

[67] Li H, Cui Q, Feng MB, Wanga J, Wenga XLJ. Applied Surface Science. 2013;**284**:179-183

[68] Anandan S, Sathish Kumar P, Pugazhenthiran N, Madhavan J, Maruthamuthu P. Solar Energy Materials & Solar Cells. 2008;**92**:929-937

[69] Suwarnkar MB, Dhabbe RS, Kadam AN, Garadkarn KM. Ceramics International. 2014;**40**:5489-5496

[70] Sobana N, Muruganadhan M, Swaminathan M. Journal of Molecular Sciences. 2006;**13**: 13275-13293

[71] Sobana N, Selvam K, Swaminathan M. Separation and Purification Technology. 2008;**62**: 648-653

[72] Chan SC, Barteau MA. Langmuir. 2005;**21**:5588-5595

[73] Lenzi GG, Fávero CVB, Colpin LMS, Bernabe H, Baesso ML, Specchia S, Santo OAA. Desalination. 2011;**270**:241-247

[74] Bo Z, Eaton RT, Gallagher JR, Canlas CP, Miller T, Notestein JM. Chemistry of Materials. 2015;**27**:1269-1277

[75] Kumar R, Rashid J, Barakat MA. Colloids and Interface Science Communications. 2015;**2**:1-4

[76] Koci K, Mateju K, Obalova L, Krejcikova S, Lacny Z, Placha D, Capek L. Applied Catalysis B: Environmetal. Review. 2010;**96**:239-244

[77] Sze CC, Barteau MA. Langmuir. 2005;**21**:5588-5595

[78] Demircia S, Dikicib T, Yurddaskal M, Gultekind S, Toparli M, Celik E. Applied Surface Science. 2016;**390**:591-601

[79] Mei S, Wang H, Wang W, Ton L, Pan H, Ruan C, Ma Q, Yang LU, Zhang L, Cheng Y, Zhang Y, Zhao L, Chu PK. Biomaterials. 2014;**35**:4255-4265

[80] Zhao L, Wang H, Huo K, Cui L, Zhang W, Ni H, Zhang Y, Wu Z, Chu PK. Biomaterials. 2011;**32**:5706-5716

[81] Asghari S, Ramezani S, Ahmadipour M, Hatami M. Designed Monomers and Polymers. 2014;**16**(4):349-335

[82] Wahyuni ET, Roto R, Prameswari M. Proceeding of the 15th International Conference on Environmental Science and Technology, August 31–September 2, 2017, Rhodes Island; 2017

[83] Chang CC, Lin C-K, Chan C-C, Hsu C-S, Chen C-Y. Thin Solid Films. 2006;**494**:274-278

[84] Lei XF, Xue XX, Yang H. Applied Surface Science. 2014;**321**:396-403

[85] Zhou Y, Kong Y, Kundu S, Cirillo JD, Liang H. Journal of Nanobiotechnology. 2012;**10**:19

[86] Ge L, Li Q, Wang M, Ouyang J, Li X, Xing MMQ. International Journal of Nanomedicine. 2014;**9**:2399-3407